The Cytosolic Class II Chaperonin CCT Recognizes Delineated Hydrophobic Sequences in Its Target Proteins†

Heidi Rommelaere,‡ Myriam De Neve,‡ Ronald Melki,§ Joël Vandekerckhove,‡ and Christophe Ampe*,‡

Flanders Interuniversity Institute for Biotechnology (VIB), Department of Biochemistry, Faculty of Medicine, University Ghent, B-9000 Ghent, Belgium, and Laboratoire d'Enzymologie et Biochimie Structurales, Centre National de la Recherche Scientifique, 91198 Gif-sur-Yvette, France

Received July 6, 1998; Revised Manuscript Received December 1, 1998

ABSTRACT: The nonhomologous proteins actin and α- and *β*-tubulin need the assistance of the cytosolic chaperonin containing TCP-1 (CCT) to reach their correct native state, and their folding requires a transient binary complex formation with CCT. We show that separate or combined deletion of three delineated hydrophobic sequences in actin disturbs the interaction with CCT. These sites are situated between residues 125−179, 244−285, and 340−375. Also, α- and *β*-tubulin contain at least one recognition region, and intriguingly, it has a similar distribution of hydrophobic residues as region 244−285 in actin. Internal deletion of the sites in actin favor a model for cooperative binding of target proteins to CCT. Peptide mimetics, representing the binding regions, inhibit target polypeptide binding to CCT, suggesting that actin and tubulin contact similar CCT subunits. In addition, we show that actin recognition by class II chaperonins is different from that by class I.

Many proteins in the cell require assistance from molecular chaperones in order to attain correctly folded states and functional conformations during protein synthesis or during recovery from the denatured state (*1, 2*). Among chaperones, the cpn60 or chaperonin family comprises multisubunit toroidal complexes that facilitate protein folding in an ATP-dependent manner. Two classes of chaperonins are distinguished on the basis of their primary structure identity (*3*). Class I contains the bacterial chaperonin GroEL, its mitochondrial counterpart Hsp60, and the Rubisco-subunit-binding protein (RBP) from chloroplasts. They all show 7-fold rotational symmetry and are composed of one (GroEL, Hsp60) or two (RBP) types of subunits. Members of class II have so far only been found in archaebacteria and in the eukaryotic cytosol. They all show 8- or 9-fold rotational symmetry (*4*−*6*). The archaebacterial chaperonins TF55 and the thermosome are composed of only two subunit species (*4, 6*), whereas the cytosolic chaperonin contains eight distinct but related polypeptides (*7, 8*), one of which is the t-complex polypeptide 1 (TCP-1) (*9, 10*). This chaperonin is therefore usually referred to as chaperonin-containing TCP-1 (CCT; other names found in the literature are TRiC and cytosolic chaperonin, ccpn). Interaction of unfolded proteins with CCT occurs in two stages. The first stage is binding of target protein to the ADP form of CCT (*11*). The second stage involves nucleotide exchange concomitant with a conformational change in the chaperonin and release of the bound protein (*11, 12*). The bound ATP is hydrolyzed after this stage to regenerate CCT in its ADP-bound form which can reenter an interaction cycle with target protein.

As yet, the requirements for interaction between chaperonins and target proteins in terms of consensus amino acid sequence, secondary structure, or the minimum length of the polypeptide chain are not fully understood, and different scenarios have been proposed on the basis of limited studies with the *Escherichia coli* chaperonin GroEL (*13, 14*). Proteolysis of unfolded rhodanese complexed to GroEL (*15*) led to a model in which GroEL contacts hydrophobic and amphipathic α-helices of approximately 60 residues in the molten globule form of rhodanese. In contrast, Clark et al. (*16*) reported that hydrophobic surface loops of about seven amino acids are the main binding determinants in murine dihydrofolate reductase (DHFR). Yet another idea is that proteins are in an extended conformation while bound to GroEL. This is based on NMR experiments of GroEL-bound cyclophilin and barnase (*17, 18*). However, other NMR experiments of nonnative α-lactalbumin, *β*-lactamase, and human DHFR bound to GroEL suggest that there may be unstable but substantial secondary structure present (*19*−*21*).

Whereas these conflicting data for target protein binding to GroEL exist, very little information is available for the recognition of nonnative proteins by CCT. Eukaryotic CCT facilitates in vitro the folding of denatured actin (*8, 9*), actin−RPV and *γ*-tubulin (*22*), and, in the presence of several protein cofactors, α- and *β*-tubulin (*8, 23*−*27*). There is evidence that next to these proteins, in vivo, other proteins are recognized by CCT (*12*). Actin and tubulin target proteins display no obvious homology; thus their interaction with

† This work was supported by the Fund for Scientific Research−Flanders (FWO−Vlaanderen) (Grants G.3008.94 and 9.0044.97 to C.A. and Grant G.0060.96 to J.V.), by the Flanders Action for Biotechnology (VLAB-COT and EC Grant Contract CHRX-CT94-0430) to J.V., and by the Association pour la Recherche sur le Cancer (ARC) and the Association Française contre les myopathies to R.M. H.R. and M.D.N. are postdoctoral fellows of the FWO and the IWT, respectively. C.A. is a research associate of the FWO.

* Corresponding author (e-mail CHAMP@gengenp.rug.ac.be, phone 0032 9 264 53 06, fax 0032 9 264 53 37).

‡ University Ghent.

§ Centre National de la Recherche Scientifique.

10.1021/bi9815905 CCC: $18.00
Published on Web 02/26/1999

CCT seems to be semispecific, and the question arises as to which features of these target proteins are important for CCT binding. In this study, we started characterizing these features by investigating the binding behavior of truncated target molecules to CCT. We here show that deletion of three delimited regions in β-actin reduces or abolishes the interaction with CCT. One region has a similar distribution of hydrophobic residues as an interaction site determined in α- and β-tubulin, suggesting that this feature is important for recognition of target proteins. Competition experiments with peptide mimetics also suggest that β-actin and tubulin contact (at least partly) similar CCT subunits. However, GroEL seems to interact in a different way with the truncated actin molecules, indicating that target protein recognition by class I and II chaperonins is distinct.

MATERIALS AND METHODS

General Methods. In vitro transcription translation reactions were carried out in a TNT T7-coupled transcription translation rabbit reticulocyte lysate system (Promega Corp., Madison, WI) in the presence of 0.02 μCi of [^{35}S]methionine (ICN Pharmaceuticals, Inc., Costa Mesa, CA) according to the manufacturers' recommendations. We analyzed the truncated translation products on 4.5% nondenaturing polyacrylamide gels (*28*) and on 15% SDS−polyacrylamide gels (*29*) in the case of the runoff assays and on 10% SDS−Tricine gels (*30*) in the case of the expressed actin constructs. Gels were stained with Coomassie blue, destained, and autoradiographed. Quantification of the ^{35}S-labeled proteins was carried out by use of a phosphorimager (Molecular Dynamics Inc., Sunnyvale, CA) and the Imagequant software package. The hydrophobicity plot of actin was calculated by the method of Eisenberg et al. (*31*).

Runoff Assays. We generated C-terminally truncated α- and β-tubulins from pET-murine α_2- and β_3-tubulin cDNA, linearized with either *Pst*I (aa 1−451), *Bst*E2 (aa 1−366), *Sty*I (aa 1−311), *Rsa*I (aa 1−260), *Xcm*I (aa 1−109), or *Sma*I (aa 1−63) in the case of α-tubulin or *Sca*I (aa 1−445), *Ava*I (aa 1−358), *Bam*HI (aa 1−343), *Nsp*I (aa 1−321), *Sac*I (aa 1−288), or *Bst*E2 (aa 1−222) in the case of β-tubulin, using a TNT coupled transcription translation system supplemented with ^{35}S-labeled methionine. We allowed the reactions to proceed for 2 h, a time sufficient to allow most of the nascent polypeptides to be released from the initial peptidyl-tRNA ribosomal complexes (*32, 33*).

Construction of Mutated Actin Proteins. We constructed C- and N-terminally truncated actin proteins by amplifying the DNA fragments encoding the amino acids, as listed in Figure 1, by PCR using β-actin full-length cDNA (*8*) as a template and primers engineered to add restriction sites for *Nco*I and *Bam*HI. We inserted the DNA fragments into the *Nco*I/*Bam*HI restriction sites of pET11d. We also constructed several internal deletion mutants of actin: (1) actinΔloop, in which the loop region (amino acids 263−272) was substituted by a glycine-threonine dipeptide sequence. This was achieved by PCR amplification of DNA fragments encoding amino acids 1−262 and 273−375 of human β-actin using primers harboring 5′ restriction sites for *Nco*I/*Kpn*I and *Kpn*I/*Bam*HI, respectively. After digestion with *Kpn*I, we ligated these two fragments and subsequently cloned them into pET11d linearized with *Nco*I/*Bam*HI; (2) actinΔM, in which

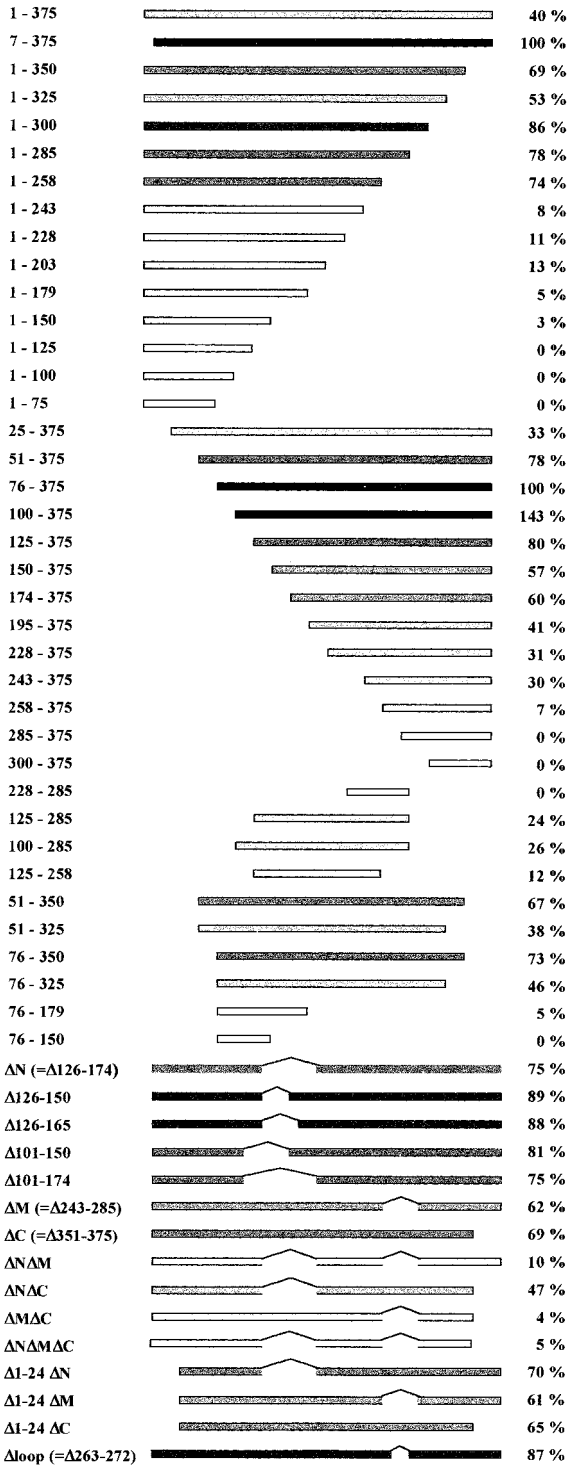

FIGURE 1: CCT binding behavior of actin mutants. The bars represent those portions of truncated actin still present as also indicated by the numbers. The connecting broken lines in the lower constructs indicate segments that are deleted (also indicated by a Δ prefix in the numbering). Percent binding indicates the relative amount of actin mutants bound to CCT, expressed as a fraction of the total amount of CCT-bound actin fragment 7−375 corrected for the expression level (as quantified from the corresponding SDS gels), and the bars are gray scale coded accordingly (darker bars indicate stronger binding). Since in reticulocyte lysate full-length actin is in a steady-state situation of binding and folding, actin could not serve as an appropriate 100% binding reference. Instead, we chose the ratio of CCT bound over total amount of fragment 7−375 as 100% reference, since this form, lacking only six residues from the N-terminus, is incapable of folding correctly and remains CCT-bound.

Table 1: Actin Peptide Mimetics: Sequences, CCT Binding, and Competition with Target Protein Binding

peptide sequences			
137−150: QAVLSLYASGRTTGC			
131−150: AMYVAIQAVLSLYASGRTTGC			
125−150: ETFNTPAMYVAIQAVLSLYASGRTTGC			
118−150: KMTQIMFETFNTPAMYVAIQAVLSLYASGRTTGC			
110−150:LNPKANREKMTQIMFETFNTPAMYVAIQAVLSLYASGRTTGC			
125−165: ETFNTPAMYVAIQAVLSLYASGRTTGIVMDSGDGVTC			
125−179:ETFNTPAMYVAIQAVLSLYASGRTTGIVMDSGDGVTHTVPIYEGYALPHAILRLD			
100−179:EHPVLLTEAPLNPKANREKMTQIMFETFNTPAMYVAIQAVLSLYASGRTTGIVMSGDGVTHTVPIYEGYALPHAILRLD			
228−260: ATAASSSSLEKSYELPDGQVITIGNERFRC			
269−285: MESAGIHETTFNSIMKC			
260−285: ALFQPSFLGMESAGIHETTFNSIMKC			
244−285:DGQVITIGNERFRAPEALFQPSFLGMESAGIHETTFNSIMKC			
334−375: RKYSVWIGGSILASLSTFQQMWISKQEYDESGPSIVHRKCF			
340−375: IGGSILASLSTFQQMWISKQEYDESGPSIVHRKCF			
356−375: CWISKQEYDESGPSIVHRKSF			
	peptide	binding to CCT	competition
N	137−150	not soluble	not tested
	131−150	not soluble	not tested
	125−150	not soluble	not tested
	118−150	not soluble	not tested
	110−150	not soluble	not tested
	125−165	not soluble	not tested
	125−179 (recombinant)	weak	yes
	100−179 (recombinant)	weak	not tested
M	228−260	no	no
	269−285	no	not tested
	260−285	weak	no
	244−285	weak	yes
C	334−375	not soluble	not tested
	340−375	weak	yes
	356−375	no	no

fragment 243−285 was deleted (PCR amplification of DNA fragments 1−242 and 286−375 with *Nco*I/*Ban*II and *Ban*II/*Bam*HI restriction sites); (3) actinΔN, in which fragment 126−175 was deleted (PCR amplification of DNA fragments 1−125 and 176−375 of β-actin with *Nco*I/*Tsp*509I and *Tsp*509I/*Bam*HI restriction sites) (the same strategy was used to construct actinΔ101−150, -Δ101−174, -Δ126−150, and -Δ126−164); (4) actinΔNΔM, in which both fragments 126−174 and 243−285 were deleted (PCR amplification of DNA fragments 1−242 and 286−375 of actinΔN with *Nco*I/*Ban*II and *Ban*II/*Bam*HI restriction sites). Actin ΔNΔC, -ΔMΔC, and -ΔNΔMΔC were created by amplifying DNA fragments encoding residues 1−350 with linearized actinΔN, -ΔM, and -ΔNΔM as template and actinΔ1−24ΔN, -Δ1−24ΔM, and -Δ1−24ΔC by amplifying DNA fragments encoding residues 25−375 with linearized actinΔN, -ΔM, and -ΔC as template, using the same strategy as for full-length β-actin. We checked the sequence of the constructs by dideoxy sequencing (*34*). We expressed the actin constructs as [^{35}S]-methionine-labeled proteins in a TNT reticulocyte T7 coupled transcription translation system (reaction time 1 h 30 min).

CCT Binding of Actin Peptide Mimetics and Competition Assay. We expressed full-length cDNAs encoding human β-actin, murine α- and β-tubulin, and actinΔloop inserted into a pET vector in *E. coli*, and we denatured these polypeptides using GuHCl and urea. We purified CCT from rabbit reticulocyte lysate as described (*9*). We chemically synthesized the actin peptides indicated in Table 1 on a model 431A peptide synthesizer using solid-phase Fmoc chemistry. We replaced internal cysteines by serines or alanines to prevent internal labeling. We carboxamidomethylated the C-terminal cysteine using [^{14}C]iodoacetamide. To monitor binding of these peptides to CCT, we incubated constant amounts of purified ADP−CCT (0.15 μM) with increasing amounts of labeled peptide (0.005−0.5 mM final concentration) during 20 min at room temperature in folding buffer (*35*). We expressed fragments 100−179 and 125−179 inserted into the pET11d vector both as ^{35}S-labeled and nonlabeled proteins in *E. coli*. We denatured these polypeptides using GuHCl and urea as described (*9*). We monitored binding of the peptides to CCT by diluting the ^{35}S-labeled protein 100-fold in folding buffer containing ADP−CCT (0.15 μM) (*9*). We further purified the nonlabeled fragments by gel filtration on a Superdex 200 column on a FPLC system (Pharmacia Biotech, Roosendaal, The Netherlands) in a buffer containing 7 M urea in 10 mM Tris-HCl, pH 7.2, and 1 mM DTT, dialyzed them against water, and concentrated them by evaporation.

For competition experiments, we added 2 μL of increasing amounts of nonlabeled peptide to 10 μL of ADP−CCT (0.15 μM) and incubated this mixture for 20 min at room temperature. Then urea-denatured ^{35}S-labeled target protein was diluted 200-fold into folding buffer containing 1 mM ATP. Immediately after dilution, we mixed 10 μL of this solution containing 2.5 pmol of target protein to the CCT−peptide mixture (0−0.28 mM final peptide concentration) and continued the incubation for 15 min. We analyzed the reaction products on 4.5% nondenaturing polyacrylamide gels in the absence of ATP and quantified the amount of target protein bound to CCT. Although we are aware that differences may exist between in vitro an in vivo folding (*33*),

we carried out the competition experiments with purified components, to avoid possible degradation of the peptide when added to a lysate system.

GroEL Binding Assay. GroEL was purified from an GroESL-overexpressing *E. coli* strain (*36*), using affinity chromatography and gel filtration as described (*37*). In vitro transcription translation reactions of actin mutants were divided in two after 20 min of incubation. The first half was left unchanged, and the second half was supplemented with purified GroEL to a final concentration of 0.5 μM. Both were incubated for an additional 40 min. The reaction products were analyzed on 4.5% native gels, according to ref *9*, which allow to wash out the hemoglobin, masking the GroEL band in the native gels according to Safer (*28*).

RESULTS

CCT Recognizes Its Target Proteins through Delimited Binding Sites. We determined the capacity of truncated target proteins to bind to CCT, with the idea that removal of parts of the sequence would result in either a gradual or an abrupt decrease in binding. A gradual loss suggests that binding information is spread over the entire length of the molecule, whereas an abrupt decrease indicates the existence of delimited binding regions. In a pilot experiment (data not shown), we monitored the binding behavior of gradually shorter ^{35}S-labeled C-terminally truncated actins in runoff assays. For this purpose, we treated cDNAs encoding β-actin with appropriate restriction enzymes. We transcribed and translated the obtained fragments in reticulocyte lysate in the presence of [^{35}S]methionine. In this experiment, also the generated mRNA pieces are truncated, and as a result, translating ribosomes will abort their action at the site corresponding to the one where the DNA was restricted, generating shorter proteins. Since the reaction occurs in reticulocyte lysate, containing endogenous CCT, the binding of these truncated molecules to CCT can be monitored readily by analyzing the reaction products on nondenaturing gels followed by autoradiography (*8*, *9*). The data from these actin runoff experiments are very similar to the data from a more detailed analysis shown below, which was designed according to two important findings we obtained from this pilot experiment.

First, we observed an increase in binding, relative to wild type, when the 39 C-terminal residues of actin were deleted, and we observed no radioactively labeled folded monomeric actin, which indicates that this truncated form is incapable of reaching a correctly folded stable conformation. Therefore, the increased binding we observed is due to a larger proportion of these truncated molecules remaining bound to CCT compared to full-length actin at steady state in the reticulocyte lysate system.

Second, we noticed a sudden and dramatic drop in the binding capacity when actin fragment 1−258 was shortened up to residue 228, indicative of local binding information. However, fragment 1−228 still possessed residual binding capacity, suggesting the presence of additional binding information in the more N-terminal part of actin. These observations hinted that delineated regions of actin are important for recognition by CCT.

Delineation of the Various Binding Regions in Actin. As the runoff approach is limited because of the availability of suitable restriction sites, we tried to delineate the regions in actin responsible for interaction in more detail using a series of designed C-terminally and N-terminally truncated actin constructs expressed as^{35}S-labeled proteins in a reticulocyte lysate system. We determined the amount of CCT-bound truncated target molecules by analyzing the reaction products on nondenaturing gels, followed by autoradiography (Figures 2a,c) and quantification by phosphorimager analysis. We measured the total amount of expressed protein by analyzing the reaction products by SDS−Tricine PAGE (Figures 2b,d). To calculate the relative binding capacities of the actin fragments, we divided the amount of CCT-bound target protein (quantified from the native gels) by the total amount of expressed protein (quantified from the denaturing gels) relative to a 100% binding reference (Figure 1).

The data obtained for the C-terminally truncated forms confirm and extend those obtained in the runoff assays mentioned above. Upon removal of the 25 C-terminal residues, binding increases compared to full-length actin, but moderately decreases compared to the 100% reference, indicating that the C-terminus of actin also contains binding information. Next, we observe again the dramatic decrease in binding capacity in the region around residue 258, and we monitor low binding from fragment 1−243 on, but it disappears when fragment 1−150 is further shortened. This is most clear when the native gels are inspected (Figure 2a) and confirms our preliminary observation of the existence of N-terminal binding information, which is probably centered around residue 150.

For the N-terminally truncated actins, we observe an important decrease in the binding capacity when fragment 7−375 is shortened to residue 25. For reasons outlined below, we think this is not due to removal of a binding site. Binding increases upon further shortening up to residue 100 and from there on decreases again (Figure 1). These data indicate that the binding information in the N-terminal part is located beyond residue 100. Another decrease in the binding occurs when fragment 243−375 is shortened up to residue 258, which confirms the data presented above. The expression level of mutant 243−375 is rather low, and hence its binding capacity might be less correctly calculated, which could imply preceding residues in the region 228−243 also contribute to the binding information of this middle region. However, if this would be the case, this contribution is minor, since the binding capacity of mutants 1−228 and 1−243 (in the C-terminally truncated constructs) is similar. In addition, peptide binding data presented below also suggest that no significant binding information is present between residues 228 and 243.

We made additional constructs truncated from both the N- and C-terminal sides (doubly truncated mutants) (Figure 1). From their binding behavior we deduced the following. The borders for the N-terminal binding information are residues 125 and 179, since no difference in binding capacity exists between fragments 100−285 and 125−285 (26% and 24%) and since binding increases from nothing to 5% by extending fragment 76−150 to 76−179 (or from no binding to 3% and 5% by extending fragment 1−125 to 150 and 179). The middle binding determinant extends up to residue 285, as binding capacity doubles when fragment 125−258 (12%) is extended up to residue 285 (24%, Figure 1). Finally, the N-terminal border of the C-terminal site seems

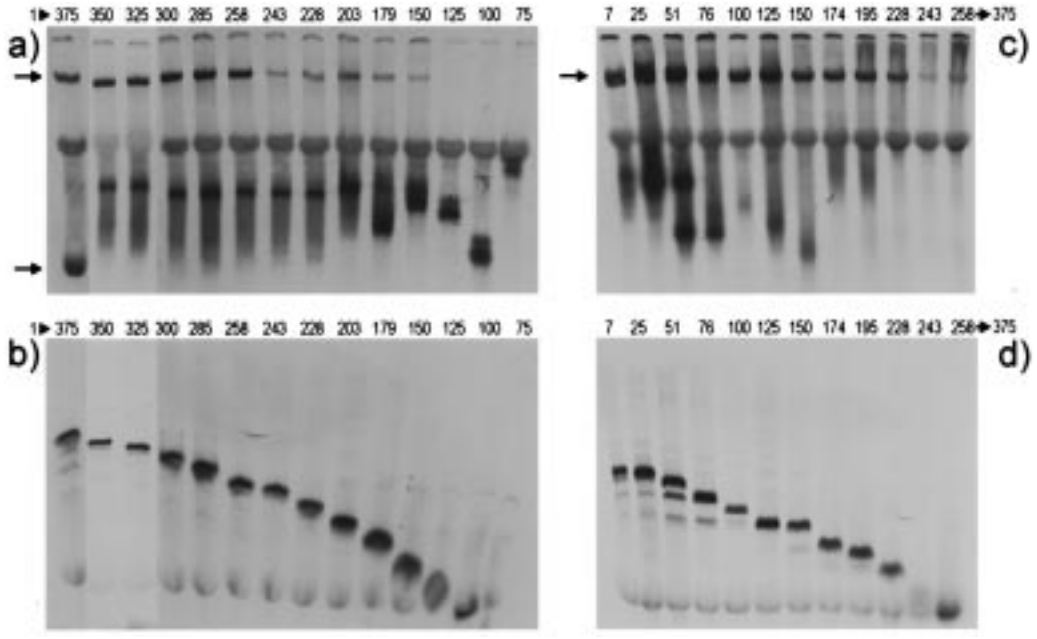

FIGURE 2: Binding behavior of truncated actin mutants to CCT indicates the presence of delimited regions with binding information. Autoradiographs of native PAGE analysis (a, c) and SDS−Tricine PAGE analysis (b, d) of in vitro transcription translation of C-terminally (a, b) and N-terminally (c, d) truncated actin mutants. The numbers on top of the gels indicate the actin fragment borders. The upper arrow in panels a and c indicates the CCT−target protein binary complex the lower arrow folded actin. The radioactive band visible in the middle of the native gels is due to translation of residual globin mRNA present in reticulocyte lysate. The radioactive band below this, observed for several of the mutants, is a complex of the actin mutant with prefoldin (*40, 41*).

to situate between residues 325 and 350, since the binding capacity of fragment 1−325 (53%) is lower than of fragment 1−350 (69%) and since binding capacity decreases upon shortening fragments 51−375 or 76−375 down to residue 325.

Thus far we have identified three different regions in actin involved in recognition by CCT: an N-terminal, a middle, and a C-terminal binding region, situated between residues 125−179, 244−285, and 325−375, respectively.

Generally, we observe that actin fragments, containing only one (or part of one) binding determinant, bind very weakly or not at all (e.g., fragments 1−150 to 1−243, 228−285, 300−375), fragments containing two determinants show respectable binding (e.g., 125−285, 243−375), and fragments containing all three determinants bind strongly (e.g., 100−375).

We note that the dramatic loss of binding capacity (70%) by C-terminal deletion of region 244−284 does not match the moderate increase when the C-terminal fragment 285−375 is extended with this region (30%) (Figure 1). Similarly, N-terminal deletion of region 125−173 results in a substantial decrease of binding (20%), while addition of this portion to N-terminal fragment 1−125 only results in low binding (5%). This strongly suggests that the various binding regions do not act independently.

To confirm the existence of the three binding sites, we used either of the two following strategies: we investigated the CCT-binding capacity of the binding regions, synthesized as separate peptides; alternatively, we checked the binding behavior of actin mutants, internally deleted from these recognition sites.

Peptide Mimetics of the Three Binding Sites of Actin Interact with CCT. Attempts to produce stable or highly labeled translation products of short fragments, representing the binding regions of actin, in lysates were unsuccessful. Therefore we used other approaches. For each determinant, we chemically synthesized several peptide mimetics covering (part of) the binding site and/or surrounding residues: peptides 110−150, 118−150, 125−150, 131−150, 137−150, and 125−165 for the N-terminal region, peptides 228−260, 244−285, 260−285, and 269−285 for the middle one, and peptides 356−375, 340−375, and 334−375 for the C-terminal site (Table 1). To monitor their ability to bind to CCT, we labeled these peptides with ^{14}C by carboxamidomethylation and subsequently incubated them with purified CCT and analyzed the reaction products on native gels. Unfortunately, all peptides mimicking the N-terminal sequence and the C-terminal peptide 334−375 are very hydrophobic and insoluble under the assay conditions used. To overcome this problem, we expressed fragments 100−179 and 125−179 as ^{35}S-labeled recombinant proteins in *E. coli*.

Incubation of the labeled material with CCT reveals that only some fragments form stable complexes with CCT. This is the case for N-peptides 100−179 and 125−179 (both bind to the same extent), M-peptides 260−285 and 244−285, and C-peptide 340−375 (Table 1). M-peptide 228−260 does not bind to CCT, again suggesting that region 228−243 contributes marginally to the middle binding determinant. In general, the binding of the peptides is weak. However, this is not surprising since, as presented above, also actin mutants possessing only one recognition determinant bind very weakly.

Internal Deletion of Binding Sites in Actin Reduces Binding to CCT. As a next step, we investigated the CCT-binding behavior of actin mutants internally deleted from one or more of the regions containing information by expressing them as ^{35}S-labeled proteins in the lysate system followed by analysis on native gels (Figures 1 and 3). Since we could not study satisfactorily the N-terminal binding site by using

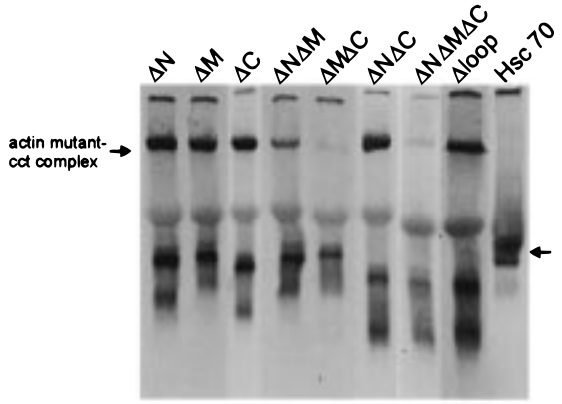

FIGURE 3: Binding behavior of internal deletion mutants of actin. Autoradiographs of native PAGE analysis of in vitro transcription translation of the single, double, and triple internal deletion mutants of actin and of Hsc70. The arrow on the left indicates the CCT−target protein complex and the one on the right folded Hsc70. For quantitative data see Figure 1.

peptide mimetics, because of their insolubility, we created various actin mutants deleted by amino acid stretches ranging from residues 100 to 174: actinΔ126−150, actinΔ126−165, actinΔ126−174, actinΔ101−150, and actinΔ101−174. Comparison of their binding capacities, shown in Figure 1, indicates that region 126−174 is close to the minimal information in the N-terminal region required for binding to CCT. This is consistent with the peptide data described above. We therefore define the actin mutant actinΔ126−174 as actinΔN that has a CCT-binding capacity of 75%.

The binding capacity of an actin mutant (actinΔM) without the middle region, 243−285, is 62%. Interestingly, this region contains a surface loop (residues 263−272) known as the "hydrophobic plug", implicated in actin filament formation (*38*, *39*). To determine the importance of this loop in the determinant, we investigated the binding behavior of an actin mutant without the loop region (actinΔloop). Its binding capacity of 87% indicates that indeed binding information is present in the loop region, since this mutant binds weaker than the 100% reference, but is certainly not restricted to it, since it binds stronger than actinΔM.

As deduced from the C-terminal deletion analysis and the peptide work, actin fragment 350−375 is close to the C-terminal binding information and fragment 1−350, referred to as actinΔC, will be used in the subsequent studies. It has a binding capacity of 69%.

Since we observed a severe decrease in binding of actin by removal of its 24 N-terminal residues, we truncated actinΔN, -ΔM, and -ΔC by their first 24 amino acids to check whether this resulted in the same effect. In these cases, however, we did not observe the severe drop (Figure 1). The aberrant binding behavior of actin N-terminally deleted by this region is thus not due to removal of binding information but might be caused by an increased binding of this mutant to prefoldin (the middle band seen on the native gels, Figure 2) (*40*). The distribution of actin mutants between the chaperones CCT and prefoldin is indicated in Table 2. For the C-terminal truncations there appears an inverse correlation between the amount of mutant bound to CCT and to prefoldin. Most of the N-terminal deletion mutants do not complex with prefoldin, suggesting that region 50−100 in the N-terminal part of actin is required for recognition by this chaperone. Prefoldin has been suggested to interact with nascent actin and tubulin chains prior to transfer to CCT (*40*). If so, the fact that N-terminal deletion mutants still bind relatively well to CCT (e.g., constructs 76−375, 100−375, and 125−375), but not to prefodin, indicates that this chaperone can be bypassed, consistent with genetic data that deletion of single prefoldin subunits in yeast or fission yeast is not lethal (*40*, *41*). Moreover, as shown above, actin fragments require the presence of at least two recognition regions to show reasonable binding to CCT; for example, fragment 1−179 containing the N-region does not bind to CCT, which argues for the fact that this part of actin contains no additional binding information. Also fragment 1−75, made as a recombinant protein, does not bind to CCT (data not shown).

To further investigate the mechanism of target protein binding to CCT and the respective contribution of the various regions, delineated by our truncation analyses, in the overall binding process, we created combined deletion mutants (Figures 1 and 3). The actin mutant with regions 126−174 and 243−285 deleted (actinΔNΔM) binds only for 10%, and a mutant without regions 243−285 and 350−375 (actinΔMΔC) binds for 4%. A combined deletion of regions 126−174 and 350−375, however, results in a mutant, actinΔNΔC, that

Table 2: Distribution of Actin Mutants between the Various Complexes Observed on Native Gels

construct	CCT bound[a]	PFD bound	third band	fourth band
reference (7−375)	68	21	11	
actin	27	3	70	
1−350	47	47	6	
1−325	36	54	10	
1−300	59	37	4	
1−285	53	43	4	
1−258	50	46	4	
1−243	5	91	4	
1−228	7	89	4	
1−203	9	87	4	
1−179	4	21	75	
1−150	2	23	75	
1−125	0	0	25	75
1−100	0	0	25	75
1−75	0	0	52	48
25−375	23	77	0	
51−375	53	26	21	
76−375	68	0	13	19
100−375	97	0	3	
125−375	75	0	25	
150−375	66	0	34	
174−375	67	0	33	
195−375	51	0	36	13
228−375	62	0	38	
243−375	36	0	64	
258−375	9	0	91	
285−375	0	0	100	
300−375	0	0	100	
ΔN	66	21	13	
ΔM	54	36	10	
ΔC	47	47	6	
ΔNΔM	18	56	26	
ΔNΔC	76	12	12	
ΔMΔC	3	76	21	
ΔNΔMΔC	8	46	46	
Δloop	54	32	14	

[a] Note that the percent CCT bound is different from the one listed in Figure 1 because the values here are not expressed relative to the reference mutant and not corrected for expression level.

still shows substantial binding (47%). ActinΔNΔMΔC (i.e., actin without its three recognition regions) only binds for 5%, which is of the same order of magnitude as actinΔMΔC. We conclude from these experiments that deletion of any binding site together with the M-site results in a dramatic drop in the binding capacity that cannot be accounted for by simply subtracting the contributions of individual binding sites. This is suggestive of a cooperative mechanism of target protein CCT interaction. When the N- or the C-site is deleted from constructs still containing the M-site, the binding capacity of the resulting protein is the result of a pure subtractive operation. These findings may point to a central role of region 243−285 (M-site) in the binding process.

Actin Peptide Mimetics Compete with Target Protein Binding to CCT. As a next step, we investigated whether the complex-forming peptide mimetics were able to compete with the binding of the typical CCT target proteins actin and α- and *β*-tubulin. Therefore, we added the ^{35}S-labeled target proteins to purified CCT, previously incubated with increasing amounts of the respective peptides.

All peptides, with exception of a shorter form (*260*−*285*) of the M-peptide, compete with all tested target proteins in a concentration-dependent manner (Figure 4). M-peptide 244−285 inhibits also the binding of actinΔloop and does this more efficiently than in the case of actin, whereas the binding of α- and *β*-tubulin is inhibited to a lesser extent by the latter and by the C-peptide. However, remarkably, regardless of the nature of the target polypeptide, we reproducibly observed an initial increase in their binding at low concentrations of added M-peptide (to a lesser extent this may also be true for the N-peptide), suggesting that the M-peptide induces a conformational change in CCT, thereby exposing the other recognition sites (see Discussion). At higher concentrations, the M-peptide efficiently competes with the CCT-bound target protein, given the strong reduction in binding capacity compared to maximal binding.

Also α- and β-Tubulin Contain Defined Regions with Information for CCT Binding. Since actin N-, M-, and C-peptides also compete with tubulins for CCT binding, these target proteins might have similar binding information as actin. To investigate this, we monitored the binding behavior of gradually shorter ^{35}S-labeled C-terminally truncated α- and *β*-tubulins in runoff assays (Figure 5). Runoff assays have proven to be reliable for quickly obtaining binding information (see above for actin and see ref *32* for *β*-tubulin). We observed analogous increases of binding for the initial truncations as in the case of shortening *β*-actin. Similarly, further deletion reduces binding dramatically: from 167% to 70%, upon shortening α-tubulin fragment 1−366 to 260 (Figure 5a) and from 211% to an amount that cannot be quantified anymore upon shortening *β*-tubulin fragment 1−321 to 222 (Figure 5b; in this case we took the ratio of CCT-bound over the total amount of full-length tubulin as a 100% binding reference). Given the homology of both tubulins, these assays indicate that binding information in these target proteins is present in the region between residues 260 and 321. This is in good agreement with, but narrows down, the binding region delineated for *β*-tubulin by Dobrzynski et al. (*32*), (residues 200 ± 50 to 350). We also observed residual binding for some of the N-terminal fragments, i.e., α-tubulin fragment 1−288 and *β*-tubulin fragment 1−109. This suggests that also in tubulins an N-terminal region with binding information exists, whereas Dobrzynski et al. (*32*) speculate on the existence of a C-terminal site, situated between residues 350 and 380.

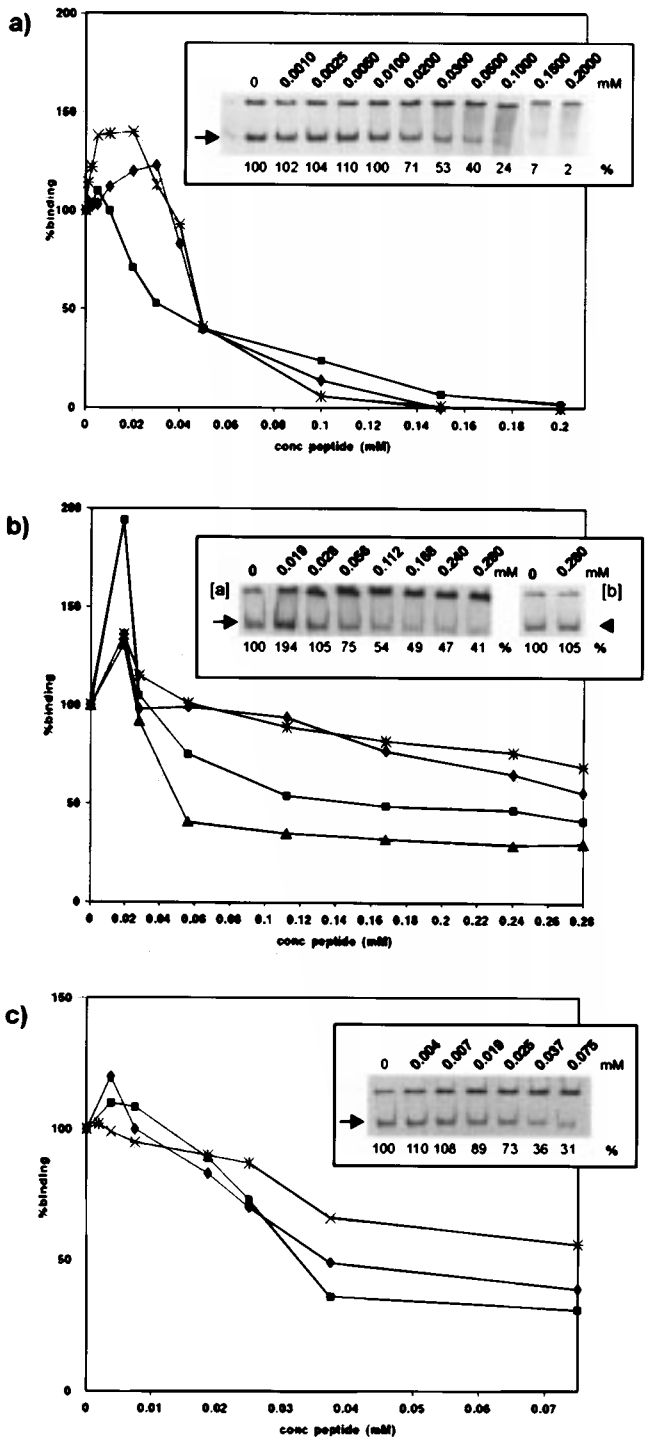

FIGURE 4: Actin peptide mimetics compete with target proteins for CCT binding in vitro. Competition between N-peptide 125−179 (a), M-peptide 244−285 (b), and C-peptide 340−375 (c) and either *β*-actin (■), α-tubulin (▲) or *β*-tubulin (*) for CCT binding. In case of the M-peptide also actinΔloop (▲) was tested. Data points represent the percentage of CCT-bound target protein, relative to the value of target protein without competing peptide, as determined from a native PAGE analysis, at the given concentrations of the peptide, shown in the inset (arrow). Inset b in panel b shows that peptide 260−285 does not compete with actin for CCT binding even at the highest concentration used. Note the difference in scale in (c). Due to the limited solubility of peptide 340−375, we were not able to use higher concentrations than 0.075 mM.

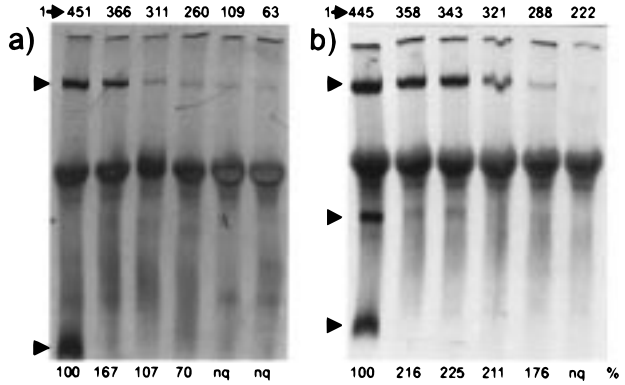

FIGURE 5: The CCT-binding behavior of truncated tubulins created in runoff assays points to the presence of delimited recognition regions in these proteins. Autoradiographs of nondenaturing PAGE analysis of runoff assays with (a) α- and (b) *β*-tubulin fragments. The length of the fragment is indicated above each lane. The upper arrow indicates the CCT−target protein complex and the lower arrow folded α- (a) or *β*-tubulin (b). The middle arrow in panel b indicates a *β*-tubulin−cofactor complex (*26*). Relative amounts of tubulin fragments bound to CCT, expressed as a fraction of the total amount of CCT-bound, full-length α- (a) or *β*-tubulin (b) corrected for the expression level (as quantified from the corresponding SDS gels, not shown), are given below each lane. It was impossible to accurately quantify (nq) the amounts of the shortest fragments bound to CCT because of very low ^{35}S levels.

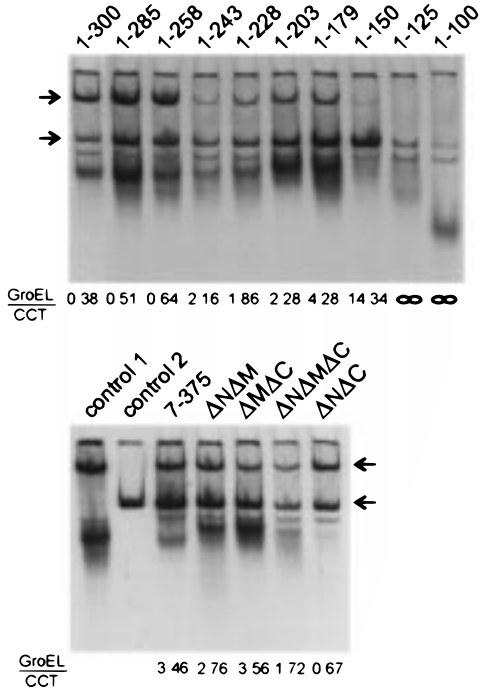

FIGURE 6: GroEL does not bind specifically to the CCT recognition regions of actin. Autoradiographs of native PAGE analysis of in vitro transcription translation reactions of actin mutants with added purified GroEL. The numbers on top of the gels indicate the actin mutants expressed; control 1 is translation of fragment 1−258 without added GroEL, and control 2 is purified GroEL incubated with ^{35}S-labeled denatured actin. The numbers below the gels represent the ratio of the amount of ^{35}S-labeled actin mutant bound to GroEL over the amount bound to CCT. Thus, high numbers indicate strong binding to GroEL. The upper arrow indicates the CCT−actin mutant complex and the lower arrow the GroEL−actin mutant complex.

GroEL and CCT Bind in a Different Manner to Actin. Although GroEL is able to bind to denatured actin, and even competes with CCT for this binding, no folded actin is released from this chaperonin (*11*, *35*). Therefore, we investigated whether GroEL interacts with the truncated actins in a similar manner as CCT. We added purified GroEL to in vitro transcription translation reactions of the C-terminally truncated actin mutants or the double or triple internally deleted mutants. Native PAGE analysis reveals that all C-terminally deleted actin mutants bind similarly to GroEL and that the sudden drops in the binding capacity upon shortening fragment 1−258 to 243 and fragment 1−150 to 125, observed for CCT, do not occur (Figure 6). The amount of actin fragments bound to GroEL relative to CCT increases upon shortening them. Also, the internally deleted mutants bind better to GroEL, with the exception of actinΔNΔC, the mutant that already shows a somewhat higher affinity for CCT (Figures 1 and 3). Thus, we can conclude that GroEL does not recognize actin via the same information regions, suggesting that the interaction of the main CCT target proteins occurs differently by class I and II chaperonins.

DISCUSSION

Actin Contains Three Regions of Binding Information for CCT, and One of These Is Similar to a Target Sequence in Tubulins. We determined the capacity of truncated actin forms to bind to CCT and showed that removal of certain parts of the sequence results in an abrupt decrease in binding. This is also the case for C-terminal truncation of segments of α- and *β*-tubulin. These observations are consistent with the idea that delimited regions in target molecules are recognized by CCT. Our truncation data for actin, combined with results obtained from analyzing the binding behavior of actin peptide mimetics and of various internal deletion mutants of actin, show that three regions in actin contain information necessary for recognition by CCT: an N-terminally located region, spanning residues 125−179, a second region, spanning residues 244−285, and a third C-terminal region, between residues 340 and 375.

This truncation analysis also reveals that the information for correct folding is not necessarily the same as information required for CCT recognition. Indeed, deletion of the first six N-terminal actin residues results in an increased CCT binding. This truncated molecule has lost its capacity to reach a correct 3D structure, since it does not coassemble with carrier actin (unpublished results). Also, *β*-tubulin deleted by its two N-terminal amino acids remains CCT arrested (*32*). This indicates that the N-terminal parts of these two CCT-target proteins are necessary for correct folding (or for stability) despite their being dispensable for binding to CCT. Xia and Peng (*42*) reported that region 356−365 plays a key role in maintaining the structural integrity of actin. This is in agreement with our observation that removal of the 25 C-terminal residues results in an increased CCT binding (compared to full-length actin) due to the incapability of this fragment of reaching a correctly folded state. Again, the same phenomenon was observed in *β*-tubulin; removal of its 27 C-terminal amino acids results in a CCT-arrested form (*32*). However, the C-terminal part of actin possesses binding information, since omitting the 25 C-terminal residues of actin results in a substantial decrease of the binding capacity, compared to the 100% binding reference, fragment 7−375.

Is Binding of the Determinants Cooperative? Our analysis of the interaction of truncated actins with CCT reveals the requirement of at least two of the three determined regions for proper binding of actin to CCT. Although we have not performed a detailed kinetic analysis, our data suggest that at least some of these sites do not act independently but in a cooperative manner. Indeed, the binding of actin mutants internally deleted by two information regions is very low (except for actinΔNΔC, Figure 3), and addition of the binding contributions of the separate N- and M-regions or M- and C-regions does not match the percentage of binding obtained for mutants that contain both N- and M-regions or both M- and C-regions. Furthermore, at low concentrations of added M-peptide, we consistently observe an increased binding of target proteins to CCT. The simplest interpretation of these observations would be that binding of the M-peptide to CCT induces a conformational change on CCT, resulting in an increase of its affinity for target proteins by exposure of other recognition sites. Thus at low concentrations of M-peptide, the target protein could interact more efficiently with CCT subunits through the other recognition determinants. Following docking of actin to the CCT binding sites, the bound M-peptide, which interacts weakly with CCT, could then easily be displaced by the actin M-determinant, when present.

According to the scenario proposed above, binding of actin determinants to CCT could be a sequential (but not necessarily a vectorial) process, in which a weak interaction between the middle determinant and CCT is established first. Following or concomitant with the binding of the N- and/or C-terminal sites, additional weak bonds between actin and CCT are generated, strengthening the interaction between actin and CCT. Such a process is also compatible with the proposal that one CCT subunit behaves as a position marker interacting with the target protein early during folding (*43*). Cooperative binding of target proteins to chaperones is not unprecedented. A similar binding mode has been hypothesized for the chaperone SecB (*44*) and for GroEL (*14, 45*), but future experiments will have to address the sequential and cooperative aspect of target protein−CCT binding.

Binding Information Appears Correlated with the Distribution of Hydrophobic Residues in the Regions Required for Recognition. In principle, the binding information in the recognition regions may be correlated with either the primary, secondary, or tertiary structure. The 3D structure of actin is known (*46, 47*), and interestingly, the N-terminal domain of Hsc70 has a similar fold (*48*). However, the latter does not require a chaperonin to reach its final 3D structure. By contrast, tubulins possess a totally different fold (*49*) and do require CCT for correct folding. Consequently, the overall fold to be reached is not a determining factor for recognition by CCT. Regular secondary structure elements, as for instance present in folding intermediates, have also been proposed as determinants for chaperonin binding, based on the suggestion that hydrophobic surfaces of α-helices in the molten globule form of rhodanese bind to GroEL (*15*). In native actin (Figure 7a) sequence 125−179 consists of a *β*-strand followed by an α-helix and two other *β*-strands, sequence 244−285 consists of a *β*-strand and a loop, known as the "hydrophobic plug" (*38, 39*), flanked by two α-helices, and sequence 340−375 consists of three α-helices. For the tubulin sequences, the regions having binding information contain two *β*-strands, an α-helix, and two loops in the native structure. If CCT recognizes regular secondary structure elements in folding intermediates, it is clear that also *β*-strands should serve as target sites. In this scenario deletion of the regions delineated above would cause a major perturbation in the local structure of the folding intermediate resulting in reduced binding. We note, however, that deletion of the 100 N-terminal amino acids at actin, thus removing a substantial part of the protein, containing folding information for the actin subdomains 1 and 2, results in increased binding to CCT. Moreover, the 44 kDa domain of Hsc70 shares similar secondary structure elements with actin in the N-terminal and middle binding region, and the former is not recognized by CCT (Figure 7b). These observations suggest that CCT does not recognize secondary structure elements and are consistent with NMR experiments showing that barnase and cyclophilin are essentially devoid of secondary structure when bound to GroEL (*17, 18*). Unfortunately, similar NMR experiments have not yet been performed on CCT-bound target proteins, so it remains to be shown whether actin and tubulins bind to CCT as folding intermediates containing local structures or through regions in an extended conformation. The latter hypothesis would indicate that binding information is present in the primary structure. It is generally accepted that the hydrophobicity plays a role in the interaction of chaperonins and their target proteins (*13, 14*). Interestingly, a hydrophobicity plot of the actin sequence shows that the positions of the most hydrophobic regions correspond to the N- and C-terminal binding information regions (Figure 7b); also the M-region displays a rather hydrophobic character. The significance of this is strengthened by our remarkable observation that the latter shows a similar distribution of hydrophobic residues as in the sequences of α- and *β*-tubulin we defined in the truncation analysis as being required for CCT binding (Figure 7b). We note, however, that these are in different secondary structure elements in the respective final 3D structures (*47, 49*). This similarity is striking since actin and tubulins are not homologous. Interestingly, the hydrophobic plug of actin has an analogous counterpart in the tubulin information region, but a similar hydrophobic loop is not present in the corresponding part of Hsc70, neither is the hydrophobic character of the flanking sequences conserved. Also, the Hsc70 sequence, corresponding to the N-site of actin, which is even more hydrophobic, shows little conservation, and the part corresponding to the C-site is almost absent. In agreement with this we could not show the formation of a binary complex between CCT and unfolded Hsc70 (Figure 3).

Although at present our data do not unambiguously allow discrimination between target protein recognition by CCT via defined regions in an extended conformation or present as nonnative folding intermediates, our data taken together with the arguments and reports cited above favor the first scenario.

Actin and Tubulins May Contact Similar CCT Subunits. It has been a puzzling observation that CCT contains eight different, but related subunits (*7, 8*), while the group I chaperonins contain only one or two (*3*). People have speculated that each subunit serves a specialized function and is involved in the assistance of folding of a particular polypeptide. We clearly show that actin N-, M-, and

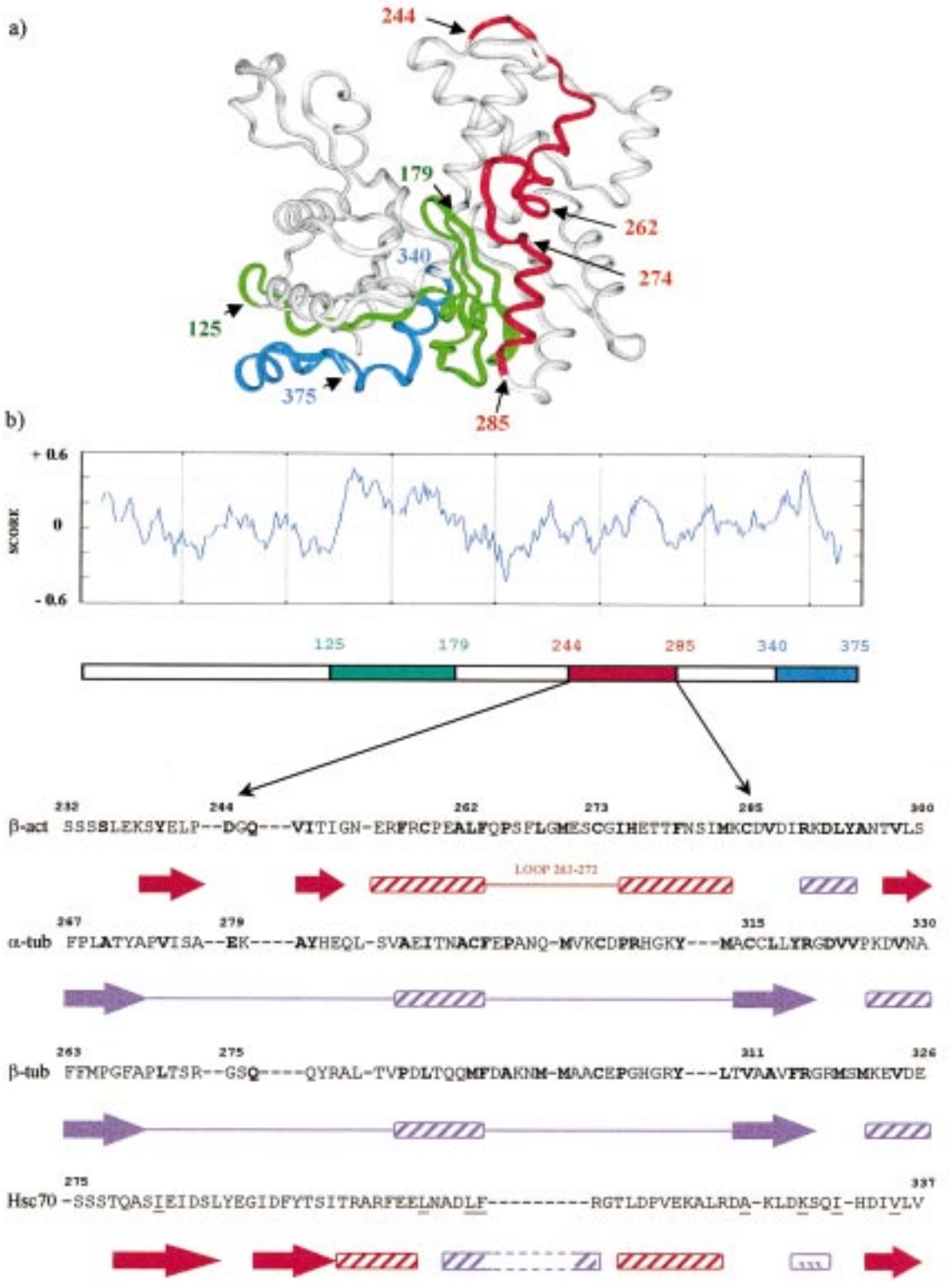

FIGURE 7: The middle region in actin has a similar distribution of hydrophobic residues as the sequence of tubulin containing information for CCT binding. Representation of the location of the three information regions, delineated in this study as being required for CCT binding, in the 3D structure of β-actin (*46*; note this is a view from, what is generally considered, the back of the molecule) (a). The N-terminal region 125−179 is shown in green, the middle region 244−285 in red, and the C-terminal region 340−375 in blue. These regions are indicated with the same color code in the primary structure of actin (b). Especially the N- and C-sites correspond well to the hydrophobic parts of actin shown in the hydrophobicity plot calculated according to Eisenberg et al. (*31*), presented with a normalized consensus hydrophobicity scale in which a positive score indicates hydrophobicity. The sequence of the middle region and flanking residues of β-actin is shown below and aligned to the determined CCT recognition regions in α- and β-tubulin and to the corresponding region of Hsc70. Residues that are identical or similar in actin and either α- or β-tubulin, or both, are in bold. In Hsc70, residues that are underlined indicate those that are identical or similar in the four proteins. The alignment of β-actin and the 44 kDa N-terminal fragment of Hsc70 is derived from ref *48*. The secondary structure elements of β-actin, tubulins (derived from ref *49*), and Hsc70 are indicated below their respective sequences: shaded cylinders indicate α-helices, cylinders labeled with 3 represent 3_{10}-helices, arrows indicate β-strands, and lines represent loops. The differences in color emphasize that the secondary structure elements in actin and tubulins are different in this region.

C-peptides compete not only with actin for binding to CCT in in vitro folding assays but also with α- and β-tubulin. The peptides probably contain nearly the minimal information required for interaction with CCT. This competition then argues for a scenario in which these target proteins bind (at least partly) to the same CCT subunits. The size we determined for the three binding determinants of actin ranges from 35 to 55 amino acids. Fragments of this size (in an extended conformation) could span two to four adjacent subunits in the CCT structure modeled on the known GroEL structure (*50*, *51*). The length of the sites is somewhat smaller than the shortest fragment of rhodanese recovered from GroEL after protease treatment of the GroEL−rhodanese complex (*15*) but considerably larger than the substrate peptides for the chaperones DnaK (*52*) and SecB (*53*) (7 and 14 amino acids, respectively). Apparently, the chaperonin subclass of molecular chaperones recognizes larger amino acid stretches in its target proteins than chaperones from the Hsp70 or SecB family.

We note that not all amino acids in the binding regions need to contact CCT. Indeed, as suggested above, the distribution of hydrophobic residues in the determinants is important for binding, and as can be seen in the middle determinant, the conserved hydrophobic residues between actin and tubulins are not clustered but dispersed along the determinant.

Nonnative Target Protein Recognition Differs for Class I and II Chaperonins. Two classes of chaperonins are distinguished on a structural basis (*3*, *50*, *54*). In addition, class I chaperonins require a cpn10 cochaperonin for proper folding of target proteins (*14*), whereas for class II chaperonins no such cochaperonin has been identified. Our results add an additional argument for the division of chaperonins in two groups. We show that GroEL, a representative of class I chaperonins, recognizes nonnative actin in a different manner than does CCT, which belongs to class II. Consistent with this is the observation that GroEL binds to unfolded actin and tubulins but, in contrast to CCT, does not release them in a native conformation (*11*, *35*). It is hypothesized that GroEL recognizes overall hydrophobicity in target proteins (*13*, *14*) and contacts them through the hydrophobic residues present in its polypeptide binding cavity (*55*). As exemplified in our study, hydrophobicity of nonnative target proteins also plays a role in class II chaperonin recognition but in addition the proper spacing of hydrophobic residues in the recognitions regions may be important. The specific distribution of these residues could then be required for the correct positioning of the information regions on the hydrophobic surface patches, which are protruding from the polypeptide-binding domains of class II chaperonins but which are absent in class I chaperonins (*54*).

ACKNOWLEDGMENT

We thank M. Goethals for peptide synthesis, V. Jonckheere for technical assistance J.-L. Verschelde for preparing the computer image of actin, and J. Zethof and Prof. Dr. Van Montagu for use of the phosphorimager.

REFERENCES

1. Gething, M.-J., and Sambrook, J. (1992) *Nature 355*, 33−44.
2. Hartl, F.-U. (1996) *Nature 381*, 571−580.
3. Kubota, H., Hynes, G., and Willison, K. (1995) *Eur. J. Biochem. 230*, 3−16.
4. Knapp, S., Schmidt-Krey, I., Hebert, H., Bergman, T., Jornvall, H., and Ladenstein, R. (1994) *J. Mol. Biol. 242*, 397−407.
5. Marco, S., Carrascosa, J. L., and Valpuesta, J. M. (1994) *Biophys. J. 67*, 364−368.
6. Phipps, B. M., Typke, D., Hegerl, R., Volker, S., Hoffmann, A., Stetter, K. O., and Baumeister, W. (1993) *Nature 361*, 475−477.
7. Kubota, H., Hynes, G., Carne, A., Ashworth, A., and Willison, K. (1994) *Curr. Biol. 4*, 89−99.
8. Rommelaere, H., Van Troys, M., Gao, Y., Melki, R., Cowan N. J., Vandekerckhove, J., and Ampe, C. (1993) *Proc. Natl. Acad. Sci. U.S.A. 90*, 11975−11979.
9. Gao, Y., Thomas, J. O., Chow, R. L., Lee, G.-H., and Cowan, N. J. (1992) *Cell 69*, 1043−1050.
10. Silver, L. M. (1979) *Cell 17*, 275−284.
11. Melki, R., and Cowan, N. J. (1994) *Mol. Cell. Biol. 14*, 2895−2904.
12. Melki, R., Batelier, G., Soulié, S., and Williams, R. C. (1997) *Biochemistry 36*, 5817−5826.
13. Coyle, J. E., Jaeger, J., Gross, M., Robinson, C. V., and Radford, S. (1997) *Folding and Des. 01*, R93−R104.
14. Fenton, W. A., and Horwich, A. L. (1997) *Protein Sci. 6*, 743−760.
15. Hlodan, R., Tempst, P., and Hartl, F. U. (1995) *Nat. Struct. Biol. 2*, 587−595.
16. Clark, A. C., Hug, E., and Frieden, C. (1996) *Biochemistry 35*, 5893−5901.
17. Zahn, R., Spitzfaden, C., Ottiger, M., Wüthrich, K., and Plückthun, A. (1994) *Nature 368*, 261−265.
18. Zahn, R., Perrett, S., Stenberg, G., and Fersht, A. R. (1996) *Science 271*, 642−645.
19. Gervasoni, P., Staudenmann, W., James, P., Gehrig, P., and Plükthun, A. (1996) *Proc. Natl. Acad. Sci. U.S.A. 93*, 12189−12194.
20. Goldberg, M. S., Zhang, J., Sondek, S., Matthews, C. R., Fox, R. O., and Horwich, A. L. (1997) *Proc. Natl. Acad. Sci. U.S.A. 94*, 1080−1085.
21. Robinson, C. V., Gross, M., Eyles, S. J., Ewbank, J. J., Mayhew, M., Hartl, F. U., Dobson, C. M., and Radford, S. E. (1994) *Nature 372*, 646−651.
22. Melki, R., Vainberg, I. E., Chow, R., and Cowan, N. J. (1993) *J. Cell Biol. 122*, 1301−1310.
23. Gao, Y., Vainberg, I. E., Chow, R. L., and Cowan, N. J. (1993) *Mol. Cell. Biol. 13*, 2478−2485.
24. Gao, Y., Melki, R., Walden, P. D., Lewis, S. A., Ampe, C., Rommelaere, H., Vandekerckhove, J., and Cowan, N. J. (1994) *J. Cell Biol. 125*, 989−996.
25. Tian, G., Huang, Y., Rommelaere, H., Vandekerckhove, J., Ampe, C., and Cowan, N. J. (1996) *Cell 86*, 287−296.
26. Tian, G., Lewis, S. A., Feierbach, B., Stearns, T., Rommelaere, H., Ampe, C., and Cowan, N. J. (1997) *J. Cell Biol. 138*, 821−832.
27. Melki, R., Rommelaere, H., Leguy, R., Vandekerckhove, J., and Ampe, C. (1996) *Biochemistry 35*, 10422−10435.
28. Safer, D. (1989) *Anal. Biochem. 178*, 32−37.
29. Laemmli, U. K. (1970) *Nature 227*, 680−685.
30. Schagger, H., and von Jagow, G. (1987) *Anal. Biochem. 166*, 368−379.
31. Eisenberg, D., Weiss, R. M., and Terwilliger, T. C. (1984) *Proc. Natl. Acad. Sci. U.S.A. 81*, 140−144.
32. Dobrzynski, J. K., Sternlicht, M. L., Farr, G. W., and Sternlicht, H. (1996) *Biochemistry 35*, 15870−15882.
33. Frydman, J., and Hartl, F.-U. (1996) *Science 272*, 1497−1502.
34. Sanger, F., Nicklen, S., and Coulson, A. R. (1977) *Proc. Natl. Acad. Sci. U.S.A. 74*, 5463−5467.
35. Tian, G., Vainberg, I. E., Tap, W. D., Lewis, S. A., and Cowan, N. J. (1995) *Nature 375*, 250−253.
36. Robbens, J. (1994) Ph.D. Thesis, University of Ghent.
37. Khandekar, S. S., Bettencourt, B. M., Kelley, K. C., and Recny, M. A. (1993) *Protein Expression Purif. 4*, 580−584.

38. Chen, X., Cook, K., and Rubenstein, P. (1993) *J. Cell Biol. 123*, 1185−1195.
39. Lorenz, M., Popp, D., and Holmes, K. C. (1993) *J. Mol. Biol. 234*, 826−836.
40. Vainberg, I. E., Lewis, S. A., Rommelaere, H., Ampe, C., Vandekerckhove, J., Klein, H. L., and Cowan, N. J. (1998) *Cell 93*, 863−873.
41. Geissler, S., Siegers, K., and Schiebel, E. (1998) *EMBO J. 17*, 952−966.
42. Xia, D., and Peng, I. (1995) *Cell Motil. Cytoskeleton 32*, 163−172.
43. Liou, A. K. F., and Willison, K. R. (1997) *EMBO J. 16*, 4311−4316.
44. Randall, L. L., and Hardy, S. J. (1995) *Trends Biochem. Sci. 20*, 65−69.
45. Zahn, R., Axman, S. E., Rücknagel, K.-P., Jaeger, E., Laminet, A. A., and Plücktun, A. (1994) *J. Mol. Biol. 242*, 150−164.
46. Schutt, C. E., Myslik, J., Rozycki, M. D., Gooneskere, N. C. W., and Lindberg, U. (1993) *Nature 365*, 810−816.
47. Kabsch, W., Mannherz, H. G., Suck, D., Pai, E. F., and Holmes, K. C. (1990) *Nature 347*, 37−44.
48. Flaherty, K. D., McKay, D. B., Kabsch, W., and Holmes, K. C. (1991) *Proc. Natl. Acad. Sci. U.S.A. 88*, 5041−5045.
49. Nogales, E., Wolf, S. G., and Downing, K. H. (1998) *Nature* 391, 199−203.
50. Braig, K., Otwinowski, Z., Hegde, R., Boisvert, D., Joachimiak, A., Horwich, A. L., and Sigler, P. B. (1994) *Nature 371*, 578−586.
51. Kim, S., Willison, K. R., and Horwich, A. L. (1994) *Trends Biochem. Sci. 19*, 543−548.
52. Zhu, X., Zhao, X., Burkholder, W. F., Gragerov, A., Ogata, C. M., Gottesman, M. E., and Hendrickson, W. A. (1996) *Science 272*, 1606−1614.
53. Randall, L. L. (1992) *Science 257*, 241−245.
54. Klumpp, M., Baumeister, W., and Essen, L.-O. (1997) *Cell 91*, 263−270.
55. Fenton, W. A., Kashi, Y., Furtak, K., and Horwich, A. L. (1994) *Nature 371*, 614−619.

BI9815905